# Combined spatial and retrospective analysis of fluoroalkyl chemicals in fluvial sediments reveal changes in levels and patterns over the last 40 years

Brice Mourier, P. Labadie, Marc Desmet, Cécile Grosbois, Julie Raux, Maxime Debret, Yoann Copard, P. Pardon, H. Budzinski, M. Babut

Author-produced version of the article published in Environmental Pollution, Volume 253, 2019, Pages 1117-1125.
doi : 10.1016/j.envpol.2019.07.079

# Combined spatial and retrospective analysis of fluoroalkyl chemicals in fluvial sediments reveal changes in levels and patterns over the last 40 years

Mourier B.[1], Labadie P.[2], Desmet M.[3], Grosbois C.[3], Raux J.[3], Debret M.[4], Copard Y.[4], Pardon P.[2], Budzinski H.[2] and Babut M.[5]

[1] Univ Lyon, Université Claude Bernard Lyon 1, ENTPE, CNRS, INRA, USC 1369, UMR5023 LEHNA, F-69518, Vaulx-en-Velin, France

[2] UMR 5805 EPOC, Université de Bordeaux I, 351 crs de la libération, F-33405 Talence

[3] Université de Tours, EA 6293 GéHCO, Parc de Grandmont, F-37200 Tours

[4] UMR 6143 – M2C, Université de Rouen, Place E. Blondel, Bat. IRESE A, F-76821 Mont St Aignan

[5] IRSTEA, RIVERLY Research Unit, Lyon-Villeurbanne Center, 5 avenue de la Doua – CS 20244, F-69625 Villeurbanne Cedex

## Research Highlights

1 - Upstream-downstream PFAS concentration gradient in bed sediments in the Rhône River

2- Reconstruction of temporal trends of PFAS contamination using a sediment core

3- Evidence of global PFSA background levels

4- Release of long-chain PFCAs from a point source into the river

5- Change of PFCA pattern through time likely reflects changes in production processes

Author-produced version of the article published in Environmental Pollution, Volume 253, 2019, Pages 1117-1125.
doi : 10.1016/j.envpol.2019.07.079

## Abstract

Bed sediments and a dated sediment core were collected upstream and downstream from the city of Lyon (France) to assess the spatial and temporal trends of contamination by per- and polyfluoroalkyl substances (PFASs) in this section of the Rhône River. Upstream from Lyon, concentrations of total PFASs (ΣPFASs) in sediments are low (between 0.19 and 2.6 ng $g^{-1}$ dry weight - dw), being characterized by a high proportion of perfluorooctane sulfonate (PFOS). Downstream from Lyon, and also from a fluoropolymer manufacturing plant, ΣPFASs concentrations reach 48.7 ng $g^{-1}$ dw. A gradual decrease of concentrations is reported at the coring site further downstream (38 km). Based on a dated sediment core, the temporal evolution of PFASs is reconstructed from 1984 to 2013. Prior to 1987, ΣPFASs concentrations were low (≤ 2 ng $g^{-1}$ dw), increasing to a maximum of 51 ng $g^{-1}$ dw in the 1990s and then decreasing from 2002 to the present day (~10 ng $g^{-1}$ dw). In terms of the PFAS pattern, the proportion of perfluoroalkyl sulfonic acids (PFSAs) has remained stable since the 1980s (~10%), whereas large variations are reported for carboxylic acids (PFCAs). Long chain- (C>8) PFCAs characterized by an even number of perfluorinated carbons represent about 74% of the total PFAS load until 2005. However, from 2005 to 2013, the relative contribution of long chain- (C>8) PFCAs with an odd number of perfluorinated carbons reaches 80%. Such changes in the PFAS pattern likely highlight a major shift in the industrial production process. This spatial and retrospective study provides valuable insights into the long-term contamination patterns of PFAS chemicals in river basins impacted by both urban and industrial activities.

## Keywords

Per- and polyfluoroalkyl substances, Rhône River, bed sediment, sediment core, temporal trend, spatial trend

## Capsule

An extended spatial and temporal survey of PFAS chemicals in sediments provided valuable insights into the long-term contamination patterns in river basins impacted by both urban and industrial activities.

Author-produced version of the article published in Environmental Pollution, Volume 253, 2019, Pages 1117-1125.
doi : 10.1016/j.envpol.2019.07.079

## 1. Introduction

Over the past 50 years, per- and polyfluoroalkyl substances (PFASs) have been widely used in the production of fluoropolymer processing additives and surfactants in industrial processes, as well as in fire-fighting foams and many consumer applications (Paul et al., 2009; Prevedouros et al., 2006). Owing to their unique properties and widespread applications, some PFASs are ubiquitously distributed in the aquatic environment (Ahrens, 2011; Ahrens and Bundschuh, 2014; Wang et al., 2015) and biota (Giesy and Kannan, 2001; Houde et al., 2011; Houde et al., 2006). This raises some concerns about the hazards PFASs might pose to wildlife or human health (Borg et al., 2013; Kannan, 2011; Naile et al., 2010; Peng et al., 2010). For PFASs currently observed in the environment, such as perfluorooctane sulfonate (PFOS) and perfluorooctanoate (PFOA), sources include direct and indirect emissions (Prevedouros et al., 2006) as well as degradation of precursors (Stock et al., 2007; Wang et al., 2009). Sediments are identified as the ultimate sink (Prevedouros et al., 2006) for PFAS having eight carbon atoms or more. Accordingly, many authors have reported the occurrence of PFASs in sediments from marine/coastal systems (e.g. (Loi et al., 2013; Theobald et al., 2011; Thompson et al., 2011), lakes (e.g. (Clara et al., 2009; Guo et al., 2016; Zhou et al., 2012) or rivers (e.g. (Möller et al., 2010; Munoz et al., 2017b; Wang et al., 2013). Sediment cores allowing the assessment of temporal trends have been studied in several contexts, such as Tokyo Bay (Ahrens et al., 2009b; Zushi et al., 2010), or in Chinese urban rivers such as the Guangzhou and Huangpu (Bao et al., 2010) or the Haihe River (Zhao et al., 2014). These studies reported different temporal trends, with a decline of “legacy” PFASs (i.e. PFOS) since the late 1990s (Ahrens et al., 2009b) or earlier (Zushi et al., 2010), while other compounds such as perfluoroundecanoate (PFUnDA) are still increasing. There is no consistent trend in Haihe river sediments, although PFOS concentrations are higher at the top of the cores than in deeper layers (Zhao et al., 2014), while cores from Guangzhou and Huangpu rivers both reveal increasing concentrations of PFOS and some perfluorocarboxylic acids (PFCAs) in the upper part of the sediment columns (Bao et al., 2010).

The Rhône is one of the largest rivers in France and represents a critical resource for agriculture and drinking water production. In Southeastern France, a peculiar PFAS molecular profile, dominated by long-chain PFCAs, is observed in fish (Miège et al., 2012) and sediments (Munoz et al., 2015) downstream from Lyon. This pattern is likely explained by an industrial source (Dauchy et al., 2012; Munoz et al., 2015).

In this context, the present study aims first to assess the spatial trends in PFAS contamination from surface sediments collected in the hydrological network around the city of Lyon, in order to identify and rank the current

Author-produced version of the article published in Environmental Pollution, Volume 253, 2019, Pages 1117-1125.
doi : 10.1016/j.envpol.2019.07.079

PFAS sources in this urban-industrial area. Then, the time trends of PFAS levels and patterns downstream of the conurbation are reconstructed though the analysis of a sediment core.

## 2. Material and methods

### 2.1 Study area

The Rhône is one of the major rivers of Europe, with a length of 810 km and a catchment area of 97 800 $km^2$ and showing a remarkable climatic and geological diversity (Pekarova et al., 2006; Desmet et al., 2005). The mean daily discharge is 1 030 $m^3$ $s^{-1}$ (1966 to 2014) downstream from its confluence with the Saône River. Along its course in French territory, the Rhône has been intensively engineered since the end of the 19$^{th}$ century, with numerous embankments, groynes and 19 dams that have been implemented for purposes of navigation, flood protection or hydroelectric production (Bravard et al., 1999). These widely-developed anthropogenic pressures have profoundly modified the hydrology and geomorphology of the Rhone valley. In addition, the Rhone passes through many urban areas and industrial zones representing localized and potential sources of contamination.

The study area was chosen to evaluate the spatial distribution and temporal trends of PFAS-contaminated sediments upstream and downstream of the Lyon metropolitan area (Fig. 1). Sediment collection sites are located in the Rhône valley upstream of the Rhône-Saône confluence, in the Saône River upstream of the confluence and along a longitudinal transect of about 38 km downstream from the Rhône-Saône confluence. This area covers the industrial corridor extending to the south of the city of Lyon, as well as several tributaries: the Ain, Bourbre and Gier. Two potential point sources of PFASs within the studied area (Fig. 1) are represented by the waste water treatment plant (WWTP) at Saint-Fons, which was seriously under-capacity until the beginning of the 2010s, and a fluoropolymer manufacturing plant that has produced various fluorinated polymers including polyvinylidene fluoride (PVDF) since the 1980s (Dauchy et al., 2012).

### 2.2 Sampling of surface sediments and flood deposits

Twenty-five samples of surface sediments were collected in July 2013 along an upstream-downstream gradient that takes into account the main Rhône tributaries and industrial areas. Table S-1 reports the geographic coordinates of sampling points as well as some field notes. Fresh flood deposits were taken from the riverbank using a stainless steel scoop, and supplemented by bed sediment sampling using an Eckman grab. Immediately after sampling, the samples were packaged and transported to the laboratory in an ice-

cooled box. In the laboratory, the samples were stored at -20°C, freeze-dried, sieved to 2 mm with a stainless steel mesh, packaged in amber glass vials and stored at room temperature until further analysis.

## 2.3 Sediment core collection and characterization

The coring site is located in a backwater area adjacent to the Rhône River, 38 km downstream from the Saône-Rhône confluence (Fig. 1). Before 1977, the side channel was not connected to the Rhône River due to river infrastructures that were implemented for navigation. After 1977, the construction of the Vaugris dam located a few kilometers downstream raised the water level and, in 1984, removal of the debris dam allowed the connection of this channel with the Rhône at its upstream end. Thus, depending on the period, the water body was connected to the main channel via its upstream and downstream ends, or solely at its downstream end.

A sediment core was sampled in June 2013 using a Uwitec gravity corer using a 2-m liner with a diameter of 63 mm operated from a specially adapted river boat (e.g. quadriraft). By means of an extension rod and weights, the corer is first gently pushed into the sediment, and then hammered until it meets resistance. Once extracted, the core is immediately conditioned in the dark and in an ice-cool box, and brought back to the laboratory the same day. The core was first visually described and then cut up at 3-cm intervals using a clean stainless steel slicer. The identified sandy layers were sampled in their entirety, and then attributed to flood-events or reconnection works on the backwater area. The separated samples were homogenized and then stored in polypropylene (PP) tubes. All samples were stored at -20°C, freeze-dried, subsequently sieved to 2 mm with a stainless steel mesh, packaged in amber glass vials and stored at room temperature until further analysis.

The grain-size distribution of the sediment core was determined with a Mastersizer 3000® laser particle size analyzer fitted with a Hydro SM small-volume dispersion unit. Percentage of particle size classes and parameters of grain size distribution were determined for each depth interval according to (Blott and Pye, 2001). Rock-Eval 6 pyrolysis was used to determine the Total Organic Content (TOC). This thermal degradation method consists of pyrolysis of a previously crushed sample, in an oven within a temperature range from 200 to 650°C, following by oxidation at 400-750°C of the pyrolysed carbonaceous residue. Each step provides an amount of OC which contributes to the cumulative TOC content of the sample (expressed in wt.%), see (Lafargue et al., 1998).

Sediment core samples were analysed for radionuclides at USGS, Menlo Park (CA, USA). Except for the three

largest sandy layers (bottom of the core), each sample was analysed for $^{226}Ra$, $^{210}Pb$, and $^{137}Cs$ using gamma spectrometry by counting for at least 24 h. Abrupt changes in grain-size identified in the cores were matched to flood discharges measured at the nearest streamflow-gauging station (Ternay, Fig. S1) or to changes following river-management operations to restore connection with the Rhône.

## 2.4 Chemicals

Certified standard solutions of analytes and internal standards (ISs) were purchased from Wellington Laboratories (via BCP Instruments, Irigny, France). Full details on the respective standard compositions are provided in the SI (section 3). Table S2 presents the list of analysed compounds, and their respective acronyms and ISs. Note that, unless otherwise stated, the PFOS concentrations presented below correspond to the sum of linear and branched isomers.

## 2.5 Extraction and Analysis of PFASs

Sediment samples (1 g dry weight, dw) were spiked with ISs and extracted by microwave-assisted extraction with methanol (5 min at 70°C) using a Start E Milestone system (Munoz et al., 2017a). Extracts were filtered through a polyethylene frit (20 µm) and concentrated to 1 mL under a nitrogen stream. Extracts were subsequently cleaned up using SuperClean Envi-Carb cartridges (250 mg, 6cc, Supelco, St Quentin Fallavier, France), the aliquots being taken down to 300 µL and then stored at -20 °C until further analysis.

The analysis of PFASs was performed by high-performance liquid chromatography coupled with tandem mass spectrometry (LC-MS/MS) using an electrospray ionization source (for full details, see Munoz et al., 2015).

## 2.6 Quality control

PFAS recovery rates were determined using sediment sample aliquots fortified at 2 ng $g^{-1}$. Actual recovery rates were determined by subtracting the analyte levels found in unspiked samples from the levels experimentally determined in the corresponding spiked samples, and were in the range 65–115 %. Procedural blanks (i.e. 10 mL of MeOH) were analysed for each samples batch (n=5). The most recurring analytes are PFHxA and PFOA, which are systematically detected in procedural blanks (0.15 ± 0.25 and 0.18 ± 0.04 ng, respectively). For these two compounds, the reporting limits are calculated as the standard deviation of blanks multiplied by the $t_{n-1.95}$ student coefficient, where n is the number of blanks (Muir and Sverko, 2006). For

Author-produced version of the article published in Environmental Pollution, Volume 253, 2019, Pages 1117-1125.
doi : 10.1016/j.envpol.2019.07.079

analytes undetected in blanks, the detection limit is defined as the concentration yielding a signal-to-noise ratio of 3 (Table 1). Limits of detection (LDs) are generally around 0.02 – 0.03 ng $g^{-1}$ (dw, dry weight).

### 2.7 Statistics

We used Pro-UCL 5.0 software (U.S. Environmental Protection Agency) to determine compound distributions accounting for left-censored results. A Mann-Whitney test was applied to compare contamination levels between groups. The significance threshold was set at 0.05 in all analyses.

## 3. Results

### 3.1 Spatial trends of bed sediment contamination

The detection rates of the 22 PFASs in bed sediment samples range from 0% for PFHxS and PFHpS, to 84% for MeFOSAA and 96 % for PFOS. Among the PFCAs, the most frequently detected compounds are PFOA (44%), PFNA (64%), PFUnDA and PFDoDA (60% each), and PFTrDA and PFTeDA (36% each). Short-chain PFCAs (i.e. PFBA, PFPeA and PFHxA) were only detected at site R4, just downstream from the fluoropolymer manufacturing plant. Table 1 reports the respective concentration ranges of the most frequently detected compounds. The full dataset of compound concentrations are provided in the SI table.

| | 6:2 FTSA | PFOA | PFNA | MeFOSAA | PFOS (Linear + Branched) | EtFOSAA | PFUnDA | PFDoDA | PFTrDA | PFTeDA | ΣPFAS |
|---|---|---|---|---|---|---|---|---|---|---|---|
| LD | 0.02 | 0.03 | 0.03 | 0.01 | 0.03 | 0.01 | 0.06 | 0.03 | 0.49 | 0.076 | - |
| Detection rate | 40% | 44% | 64% | 84% | 96% | 56% | 60% | 60% | 36% | 36% | - |
| 1st quartile | 0.02 | 0.03 | 0.03 | 0.02 | 0.51 | 0.01 | 0.06 | 0.03 | 0.49 | 0.076 | 0.75 |
| median | 0.02 | 0.03 | 0.18 | 0.03 | 0.65 | 0.01 | 0.32 | 0.10 | 0.49 | 0.076 | 1.77 |
| 3rd quartile | 0.13 | 0.15 | 0.40 | 0.05 | 0.80 | 0.03 | 0.86 | 0.24 | 3.72 | 0.468 | 5.73 |
| maximum | 1.09 | 1.05 | 2.70 | 1.20 | 2.10 | 2.86 | 5.32 | 2.30 | 20.9 | 4.35 | 49.3 |

**Table 1 – Distributions of PFASs (n=25) most frequently detected in bed sediments and flood deposits (ng $g^{-1}$ dw)**

The molecular profiles in bed sediment sharply changes from upstream to downstream of site R4: for instance, detection rates of 6:2 FTSA, PFNA and PFTrDA increase from 0% to 69 %, from 18 % to 100%, and from 0% to 61%,respectively. PFOS detection rates are not affected, while MeFOSAA and EtFOSAA show a moderate

200 variation, with detection rates of 72.7% to 92.3% and 45.5% to 61.5%, respectively. The respective proportions
201 of compounds are quite different between river stretches (Fig. S2). PFOS is predominant in the Saône River
202 sediments (Fig. S2-A), as well as in other tributaries (Fig. S2-B in SI). Some PFCAs, i.e. PFNA, PFUnDA and
203 PFDoDA, are present in moderate proportions in some samples from the tributaries (S2, B1, G1), but not in
204 samples from the Rhône River upstream of site R4, except in one case where the PFCAs, in particular long-
205 chain PFCAs (N perfluorinated C atoms ≥ 8), as well as PFDoDA, are predominant downstream from site R4
206 (Fig. S2-D in SI). These compounds represent 99 to 100% of ΣPFCAs at all sites, except at R4, which is the
207 only site where short-chain carboxylates were detected as mentioned above. Meanwhile, as shown on Fig. 1,
208 PFCA concentrations increase significantly from up- to downstream of R4, even when this site is ignored as
209 an outlier. Conversely, the concentrations of PFOS and its precursors remain similar (Mann-Whitney, *p*-value
210 = 0.95), despite locally higher concentrations at sites R4 and R5 (Fig. S3 in SI). PFCA concentrations tend to
211 decrease gradually downstream from site R4 to site R9, although not linearly. This is probably a consequence
212 of complex hydro-sedimentary processes along the investigated river stretches (Fig. 1, Fig. S4 in SI). In
213 addition, 6:2 FTSA is undetected upstream from site R4 (Fig. S2-C), while it is generally detected in Rhône
214 River bed sediments downstream from this site (concentrations ranging between 0.02 and 1.09 ng $g^{-1}$ dw), but
215 not in samples from the Gier river: this strongly suggests the existence of a local source close to site R4.
216

Author-produced version of the article published in Environmental Pollution, Volume 253, 2019, Pages 1117-1125.
doi : 10.1016/j.envpol.2019.07.079

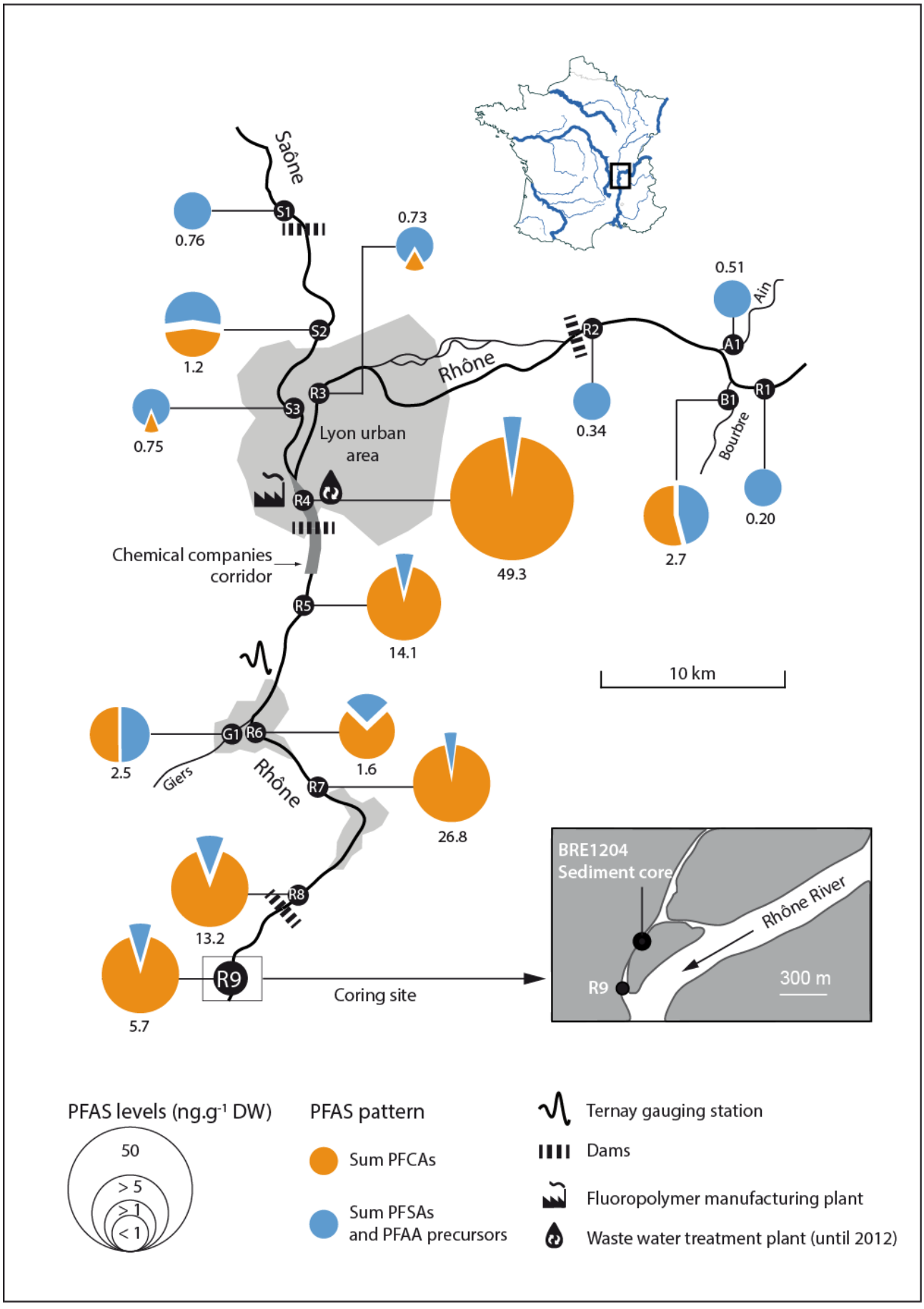

**Figure 1 – PFAS contamination of sedimentary deposits (ng $g^{-1}$ dw) collected in the drainage network of the Lyon area (France). To simplify the data presentation, PFOS precursors and 6:2 FTSA are grouped into perfluoroalkyl acid (PFAA) precursors. Blue segments represent the sum of PFSAs and PFAA precursors; orange segments correspond to the sum of PFCAs. When several samples are available for a given site, we use the arithmetic mean of the respective measurements.**

In a few cases, several kinds of sediment sample (i.e. dry deposits, wet deposits or bed sediments) are available from the same location. These samples provide similar records of ΣPFASs contamination, except at site R5.2, where there is a discrepancy of 5 ng $g^{-1}$ in ΣPFASs concentrations on a dry weight basis between wet and dry deposits (Fig. S5 in SI).

In summary, this survey shows (i) multiple sources of PFSAs and PFOS precursors along the investigated river stretches, (ii) a local discharge of both short-chain (PFHxA) and long-chain (PFNA, PFUnDA, PFTrDA) PFCAs related to a fluoropolymer production platform, as well as (iii) another local discharge of 6:2 FTSA, Me-FOSAA and Et-FOSAA, probably from a WWTP.

## 3.2 Sediment core

### 3.2.1 Core description and characterization

The 140-cm sediment core is characterized in terms of its visual description, grain-size distribution and TOC content. The sediment consists of light-grey sand in the lower part of the core and homogenous brown silt interrupted by event-layers in the upper part. Three sedimentary units are distinguished (Fig. 2). The bottom unit (Unit I) includes three thick sandy intervals at 93-106 cm, 108-119 cm and 134.5-141 cm (D50 of 337, 366 and 444 µm, respectively). These deposits have a low TOC content (<0.5%). Between 119 and 134.5 cm, the sediments are uniformly fine-grained with TOC contents close to 1%. An increase of fine particles and TOC content is observed between 86 and 93 cm. Unit II includes silty deposits (D50 of 18.8 ± 4.0 µm) interrupted by 5 layers characterized by their coarser grain size (D50 of 151.5 ± 87.2 µm). The TOC content is 1.8 ± 0.2% in the silty deposits, whereas it drops to 0.9 ± 0.8% in coarser layers. The uppermost unit (Unit III) includes silty deposits with grain size decreasing upward. Finally, the TOC content ranges between 1.6 and 2% at the bottom of Unit III and is marked by an increase to almost 3% at the top of the core.

Author-produced version of the article published in Environmental Pollution, Volume 253, 2019, Pages 1117-1125.
doi : 10.1016/j.envpol.2019.07.079

### 3.2.2 Dating

The date of deposition of the sediments is estimated on the basis of the $^{137}$Cs profile and by correlating changes in grain-size distribution in the sediment cores to the timing of flood events as well as major changes at the site (Fig. 2). The radionuclide profile of the core yields a calibrated date at 107 cm (Fig. 2), corresponding to the $^{137}$Cs fallout resulting from the Chernobyl accident in 1986 (Anspaugh et al., 1988). The sudden change in grain-size distribution in U1, associated with the occurrence of two thick sandy layers, is interpreted as corresponding to debris removal works carried out in 1984 which re-established the connection to the Rhône as already shown by Desmet et al. (2012). This event is consistent with the radionuclide profile. Flood-event deposits are matched to flood discharges measured at the nearest streamflow-gauging station (Ternay, Fig. S1-A). Five major flood events (defined as $Q_{10}$>4200 m3 $s^{-1}$) identified in the core are dated in the early 1990s and 2000s (Fig. S1-B). Since November 2002, no major flood has been recorded at the Ternay station. By matching dated flood facies with removal work facies and the $^{137}$Cs peak, an age-depth model can be calculated, assuming a constant deposition rate between two successive date markers. Prior to 1984, we assume that this site was not directly connected to the Rhône River.

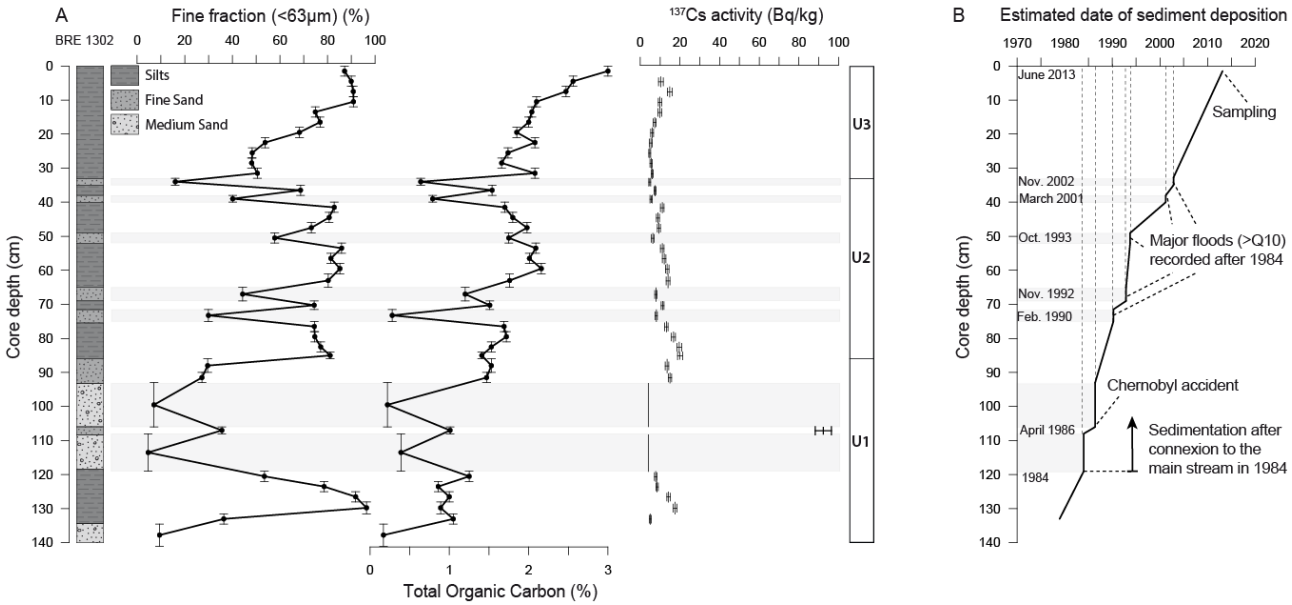


**Fig. 2. A/ Profiles of fine fraction (<63 µm), total organic carbon (TOC, %) and $^{137}$Cs activity (Bq/kg) in BRE1202 sediment core. B/ Date of sediment deposition estimated on the basis of $^{137}$Cs profile and variations in grain size matched with flood events and works for reconnection to the river.**

3.2.3 PFAS concentrations and molecular patterns

Figure 3 shows the temporal trends of PFASs in the sediment core and the full dataset of compound concentrations are provided in the SI. Values are expressed in terms of dry weight as well as on a TOC-normalized basis since Organic Carbon (OC) is a major factor affecting PFAS sorption onto sediments (Higgins and Luthy, 2006 ; Munoz et al., 2015).

Five compounds are detected among the sulfonates and PFOS precursors: PFOS, FOSA, MeFOSA, EtFOSA as well as 6:2 FTSA. Their frequency of detection (or detection rate) ranges from 85 to 100 %. The maximum concentration of PFOS and its precursors was attained between 1988 and 2002 (maximum concentration of 2.3 ng $g^{-1}$ dw or 134.3 ng $g^{-1}$ OC at the end of 1993); a similar trend is observed for 6:2 FTSA, with a maximum concentration of 0.88 ng $g^{-1}$ dw (or 43.6 ng $g^{-1}$ OC) in the sediment layer deposited in 1993. In terms of compound profiles, the maximum relative contribution of sulfonates and PFOS precursors is observed before 1988, accounting for 10–60% of ΣPFASs. In the 1988– 2013 sediment interval, the relative contribution of the same compounds lies in the range 4 –15%.

Ten PFCAs can be detected in the sediment core samples. In sediments deposited before 1988, the detection frequencies range from 0 to 36%, with exceptions for PFPeA (100%), PFDA (82%) and PFDoDA (91%). Nevertheless, the detection rates for all samples are relatively high and range between 75 and 98 %, except for short-chain PFCAs such as PFHxA (30%), PFHpA (58 %) and PFOA (43. In addition, PFOA and PFHpA show a maximum frequency of detection between 1988 and 2003, while PFPeA is detected in 98% of samples in sediment layers deposited over this time interval. The maximum concentration for PFCAs is recorded in 1993 for 6 compounds (PFHpA, PFOA, PFNA, PFDA, PFDoDA and PFTeDA), and this sediment interval also coincides with the maximum concentration of ΣPFASs (51.4 ng $g^{-1}$ dw or 2459 ng $g^{-1}$ OC). PFHxA, PFUnDA and PFTrDA reach their maximum levels in the most recent layers (2010s).

When considering the three sedimentary units described above, the following conclusions can be drawn:

(i) Unit 1 – (< 1988): the average concentration of ΣPFASs is 3.4 ± 4.0 ng $g^{-1}$ dw and is dominated by carboxylates (PFPeA, PFOA and PFDA) and 6:2 FTSA, while the contribution of PFOS is lower than 8%;

(ii) Unit 2 (1988-2003): the average concentration of ΣPFASs is 20.3 ± 15.1 ng $g^{-1}$ dw. The PFAS molecular pattern is dominated by long-chain PFCAs, especially compounds with an odd fluorinated carbon number (PFDA, PFDoDA and PFTeDA) which conjointly account for 59 – 85% of ΣPFASs;

(iii) Unit 3 (2003-2013): the average concentration of ΣPFASs is 9.8 ± 4.7 ng $g^{-1}$ dw and is lower than in unit 2. The PFAS molecular pattern is still dominated by long-chain PFCAs, but a rapid decrease is observed in

Author-produced version of the article published in Environmental Pollution, Volume 253, 2019, Pages 1117-1125.
doi : 10.1016/j.envpol.2019.07.079

the relative abundances of long-chain PFCAs with an odd fluorinated carbon number, while long-chain PFCAs with an even fluorinated carbon number progressively become predominant (e.g. PFUnDA and PFTrDA account for up to 75 % of ΣPFASs in the most recent sediment layers).

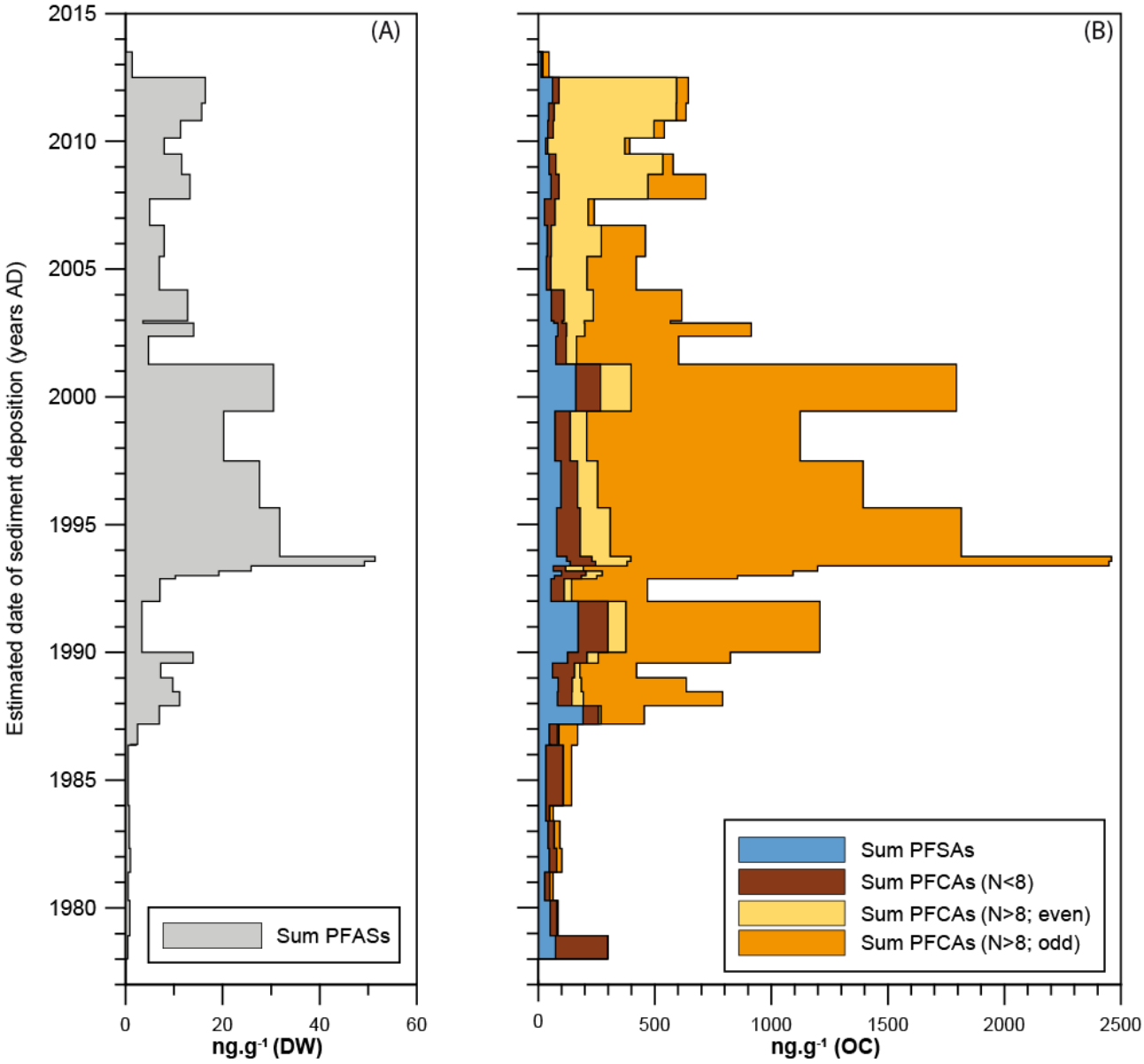


**Figure 3 Temporal evolution of the total concentration of PFASs (A) and OC-normalized concentrations of four PFASs groups (B): sum of PFSAs and PFOS precursors (6:2 FTSA included); sum of short-chain PFCAs; sum of long-chain PFCAs with an even number of perfluorinated carbon atoms; sum of long-chain PFCAs with an odd number of perfluorinated carbon atoms.**

## 4. Discussion

### 4.1 PFAS sources

In terms of PFAS levels, there is a clear spatial trend between sediments collected upstream and downstream of industrial and urban areas of the city of Lyon. PFOA and PFOS distributions appear similar to those observed in other urban/industrialized regions (e.g. (Bečanová et al., 2016; Myers et al., 2012; Zhao et al., 2014), while long-chain PFCAs (especially PFUnDA, PFDoDA, PFTrDA and PFTeDA) display unusually high levels and relative abundances at site R4 and further downstream, as already noted by Dauchy et al. (2012) and Munoz et al.(2015). 6:2 FTSA is not detected in sediments upstream from site R4, while it is found in most samples collected downstream. Together with other potential precursor degradation products (e.g. MeFOSAA and EtFOSAA), this compound has been frequently identified downstream of WWTPs (Ahrens et al., 2009a) or industrial plant (Dauchy et al., 2017).

We therefore conclude that PFASs contamination in the upstream part of the study area results from a complex combination of multiple point and non-point sources. The molecular patterns observed in this area are similar to those previously reported in a wide variety of settings across French fluvial systems (Munoz et al. 2015). In this latter study, PFOS is found to be the prevalent compound, accounting for between 34 and 100% of ΣPFASs. The large increase in concentrations downstream of site R4 indicates substantial inputs of PFASs to the Rhône River via local point sources such as the fluoropolymer manufacturing plant. Another potential sources of 6:2 FTSA and PFOS precursors include the St-Fons WWTP (~$10^6$ population equivalents) and the Gier River, a well-documented tributary affected by industrial activities (Poulier et al., 2019) where sediments show one of the highest concentrations reported in this study for bed sediments or deposits (>$90^{th}$ percentile of ΣPFSAs). As regards long-chain PFCAs, the increase in PFNA, PFUnDA and PFTrDA is very probably related to inputs from the fluoropolymer production plant, which is consistent with the results of Dauchy (2012). PFNA was actually used as a processing aid in fluoropolymer synthesis (e.g. polyvinylidene fluoride, PVDF). PFUnDA and PFTrDA likely represent impurities of the ammonium perfluorononanoate (APFN) used for industrial applications (Buck et al., 2011).

### 4.2 Influence of deposition patterns on PFAS concentrations in the sediment core

Floods and river-management operations have affected sediment deposition patterns at the sediment core site. Sediments deposited just after the debris dam removal in 1984 are assumed not to represent the same depositional conditions as recorded in more recent intervals. Indeed, sandy and well-sorted intervals in the deepest part of the core contrast with fine-grained and poorly classified sediments deposited in the upper part of the core. Such changes in the connectivity conditions that control deposition processes might also explain

some short-term variations in the vertical profile of PFASs. Major flood events occurring in the early 1990s and 2000s, result in lower PFAS levels as reflected by increased sand content and a decrease in organic carbon content in some core layers. The relatively low total PFAS concentration measured in the most recent sample (1.4 ng $g^{-1}$ dw) indicates a possible dilution effect attributed to upstream sediment flushing that occurred in 2012, just before coring operations.

ΣPFAS concentrations appear to decrease in each layer corresponding to a flood event. This is consistent with (Ahrens et al., 2011), who showed a lower sorption capacity for sandy sediment with a low TOC content, whereas higher sorption capacities are found for muddy sediments with higher TOC content. When normalized according to OC content, PFAS concentrations in flood layers converge with the values measured in adjacent layers. Similarly, the apparent increase of PFAS concentrations in the upper part of the core is mainly due to a change in OC content in these layers. However, considering OC-normalized concentrations, there is no significant change in concentrations of ΣPFAS from about 2008 to layers from the top of the core dated at 2013 (Kendall's tau test of correlation, p=0.45).

### 4.3 Temporal trend in the sediment core and comparison with sediment cores worldwide

Numerous studies have been published during the last decade using sediment cores for assessing the spatial or temporal trends of PFAS contamination (e.g. (Ahrens et al., 2009b; Bao et al., 2009; Codling et al., 2018a; Codling et al., 2018b; Codling et al., 2014; Yeung et al., 2013). These studies differ in several ways, such as objectives, dating methods and range of analysed compounds. Some studies have targeted remote lakes to elucidate PFCA atmospheric pathways to these areas (Benskin et al., 2011), while others have dealt with large water bodies in industrialized regions to better understand PFAS fate and observe the effects of production using changes at a large spatial scale (Myers et al., 2012; Zushi et al., 2010). Several studies have focused on river stretches or lake sections directly influenced by industrial parks (Zhao et al., 2014; Zhou et al., 2013) or cities (Bao et al., 2010). Sediment sample dates were either not determined, or estimated using a range of radionuclides ($^{210}$Pb, $^{137}$Cs, $^{241}$Am).

The range of PFASs analysed in these studies varies from a few PFCAs to large sets of compounds including PFSAs, FTSAs, FOSAs and FOSAAs; only few studies normalize PFAS concentrations to TOC content (Zhou et al., 2013; Zushi et al., 2010), making it impossible to directly compare contamination levels. It would be more reasonable, however, to use indicators such as ΣPFASs, ΣPFCAs or ΣPFSAs as trend indicators,

provided the range of analysed compounds is large enough, because they would account for changes in production processes, e.g. from PFOS to shorter chain PFSAs, and for degradation of precursors into PFCAs (Benskin et al., 2011) or PFOS (Zushi et al., 2010). ΣPFASs or ΣPFCAs/PFSAs trend patterns as well as the period of maximum concentration (peak date) could therefore provide information about such changes.

In the Rhône River, the increase of ΣPFASs in the 1990s (up to 51.4 ng $g^{-1}$ dw in 1994), was followed by a decrease in concentrations (to ~10 ng $g^{-1}$ dw), which have remained stable since the late 2000s. Overall, the molecular profile is largely dominated by long-chain PFCAs. Moreover, a shift is observed from odd to even perfluorinated carbon atom numbers: PFDA and PFDoDA were dominant before 2002, (i.e. mean contributions to ΣPFCAs of 37% and 31%, respectively), while PFUnDA and PFTrDA represent the highest contributions (29 and 45% of ΣPFCAs, respectively) in the post-2005 deposits. This shift is very likely related to changes in the production process at the industrial plant, as already mentioned in similar contexts (Zhou et al., 2013). Such a trend is similar to that in Tokyo Bay cores, where long-chain PFCA concentrations (e.g. PFUnDA and PFTrDA) have been continuing to increase at the top of the cores since 2005 (Ahrens et al., 2009b; Zushi et al., 2010). A similar increase of long-chain PFCA concentrations was also reported in Lake Ontario (Myers et al., 2012) as well as in some other Laurentian Great Lakes (Codling et al., 2018a). Nevertheless, published data on long-chain PFCAs in cores show either increasing trends (Bao et al., 2010; Gao et al., 2014; Yeung et al., 2013; Zhao et al., 2014) or indeterminate trends (Codling et al., 2018a; Codling et al., 2018b).

The PFOS trend in the Rhône River core is not obvious, as concentrations vary a great deal over the years, even when normalized to OC. There are nevertheless three distinct periods (Fig. S6): before ca. 1985, PFOS concentrations remain below 15 ng $g^{-1}$ OC. During the next period (1985-2000), PFOS concentrations range between 20 to 60 ng $g^{-1}$ OC, whereas OC-normalized concentrations range between 20 and 40 ng $g^{-1}$ OC in the most recent layers (since the years 2000). After exclusion of the two outliers measured in 1987 and 1999, PFOS concentrations normalized to OC content are significantly (Mann-Whitney, $p$=0.028) higher during the 1985-2000 period compared to the most recent period (with respective means of 35.9 and 25.4 ng $g^{-1}$ OC), indicating a downwards shift after 2002. Similar shifts are also noted in other parts of the world, e.g. Tokyo Bay in Japan (Ahrens et al., 2009b) or Lake Michigan (USA) (Codling et al., 2014), as well as Lake Ontario (Canada) (Myers et al., 2012), owing to the withdrawal of PFOS from industrial applications (Paul et al., 2009), and thus their reduced levels in consumer products (Boulanger et al., 2005). Interestingly, in the abovementioned Lake Ontario study, the suspended sediment from its main tributary, the Niagara River, responded rapidly to the phase-out of PFOS, with a concentration drop in 2000, while PFOS concentrations

were still increasing at the top of the sediment cores (middle of the lake) in 2006. Sediment records from riverine systems, such as the Niagara and Rhône rivers, might accordingly track the consequences of contaminant phase-out more rapidly compared with large lakes.

## 5. Conclusion

The Rhône River upstream and downstream from Lyon is subject to multiple sources of emission of perfluoroalkyl substances, generating a complex pattern of sediment contamination. An extended spatial survey of flood and bed sediments reveals multiple sources of PFSAs and PFOS precursors, as well as local discharges of short-chain (PFHxA) and long-chain (PFNA, PFUnDA and PFTrDA) PFCAs, 6:2 FTSA and FOSAAs. Based on the analysis of a sediment core collected in a secondary channel 38 km downstream from the local discharge, we show that industrial emissions of PFAS became quite significant by the late 1980s, reaching a maximum in the 1990s (maximum recorded ΣPFASs: 51.4 ng $g^{-1}$ dw in 1994). During this period, PFDA, PFDoDA and PFTeDA provided the main contribution (74%) to ΣPFASs. From ca. 2005 onwards, concentrations decreased to a plateau, but were still influenced by local inputs and activities. The molecular profile of PFCAs in the sediment column shifted from an odd to even number of fluorinated carbon atoms, PFTrDA and PFUnDA representing about 75% of ΣPFASs in sediment core samples after 2005. Such a compositional shift strongly suggests that changes occurred in the production process of the industrial plant. PFASs concentrations measured in this sediment core appear to be amongst the highest recorded in sediment cores worldwide. This spatial and retrospective study provides valuable insights into the long-term contamination patterns of PFAS chemicals in river basins impacted by both urban and industrial activities.

## Acknowledgments

This study was funded by the Rhône-Mediterranean and Corsica Water Agency and the Rhône-Alps Region in the context of the Rhône River ecological restoration plan. We thank Raphael Barlon and the team of the "Centre d'Observation de l'Ile du Beurre" (Tupins & Semons, France) for their support in core collection. We also thank Fanny Arnaud for providing us hydrological data from the Ternay gauging station as well as Christopher Fuller and Peter Van Metre (both at USGS) for fruitful discussions. The Aquitaine Region and the European Regional Development Fund are also acknowledged for their financial support (CPER A2E). This study was carried out with financial support from the French National Research Agency (ANR) in the framework of Investments for the future Program, within the Cluster of Excellence COTE (ANR-10-LABX-45). Dr. M.S.N. Carpenter post-edited the English style and grammar.

Author-produced version of the article published in Environmental Pollution, Volume 253, 2019, Pages 1117-1125.
doi : 10.1016/j.envpol.2019.07.079

431

## References

Ahrens, L., 2011. Polyfluoroalkyl compounds in the aquatic environment: A review of their occurrence and fate. Journal of Environmental Monitoring 13, 20-31.
Ahrens, L., Bundschuh, M., 2014. Fate and effects of poly- and perfluoroalkyl substances in the aquatic environment: A review. Environmental Toxicology and Chemistry 33, 1921-1929.
Ahrens, L., Felizeter, S., Sturm, R., Xie, Z., Ebinghaus, R., 2009a. Polyfluorinated compounds in waste water treatment plant effluents and surface waters along the River Elbe, Germany. Marine Pollution Bulletin 58, 1326-1333.
Ahrens, L., Yamashita, N., Yeung, L.W.Y., Taniyasu, S., Horii, Y., Lam, P.K.S., Ebinghaus, R., 2009b. Partitioning Behavior of Per- and Polyfluoroalkyl Compounds between Pore Water and Sediment in Two Sediment Cores from Tokyo Bay, Japan. Environmental Science & Technology 43, 6969-6975.
Ahrens, L., Yeung, L.W.Y., Taniyasu, S., Lam, P.K.S., Yamashita, N., 2011. Partitioning of perfluorooctanoate (PFOA), perfluorooctane sulfonate (PFOS) and perfluorooctane sulfonamide (PFOSA) between water and sediment. Chemosphere 85, 731-737.
Bao, J., Jin, Y., Liu, W., Ran, X., Zhang, Z., 2009. Perfluorinated compounds in sediments from the Daliao River system of northeast China. Chemosphere 77, 652-657.
Bao, J., Liu, W., Liu, L., Jin, Y., Ran, X., Zhang, Z., 2010. Perfluorinated compounds in urban river sediments from Guangzhou and Shanghai of China. Chemosphere 80, 123-130.
Bečanová, J., Komprdová, K., Vrana, B., Klánová, J., 2016. Annual dynamics of perfluorinated compounds in sediment: A case study in the Morava River in Zlín district, Czech Republic. Chemosphere 151, 225-233.
Benskin, J.P., Phillips, V., St.Louis, V.L., Martin, J.W., 2011. Source Elucidation of Perfluorinated Carboxylic Acids in Remote Alpine Lake Sediment Cores. Environmental Science & Technology 45, 7188-7194.
Blott, S.J., Pye, K., 2001. GRADISTAT: A grain size distribution and statistics package for the analysis of unconsolidated sediments. Earth Surface Processes and Landforms 26, 1237-1248.
Borg, D., Lund, B.-O., Lindquist, N.-G., Håkansson, H., 2013. Cumulative health risk assessment of 17 perfluoroalkylated and polyfluoroalkylated substances (PFASs) in the Swedish population. Environment International 59, 112-123.
Boulanger, B., Vargo, J.D., Schnoor, J.L., Hornbuckle, K.C., 2005. Evaluation of perfluorooctane surfactants in a wastewater treatment system and in a commercial surface protection product. Environmental Science and Technology 39, 5524-5530.
Clara, M., Gans, O., Weiss, S., Sanz-Escribano, D., Scharf, S., Scheffknecht, C., 2009. Perfluorinated alkylated substances in the aquatic environment: An Austrian case study. Water Research 43, 4760-4768.
Bravard, J.-P., Landon, N., Peiry, J.-L., Piégay, H. 1999.Principles of engineering geomorphology for managing channel erosion and bedload transport, examples from French rivers. Geomorphology 31, 291-311. https://doi.org/10.1016/S0169-555X(99)00091-4
Codling, G., Hosseini, S., Corcoran, M.B., Bonina, S., Lin, T., Li, A., Sturchio, N.C., Rockne, K.J., Ji, K., Peng, H., Giesy, J.P., 2018a. Current and historical concentrations of poly and perfluorinated compounds in sediments of the northern Great Lakes – Superior, Huron, and Michigan. Environmental Pollution 236, 373-381.

Codling, G., Sturchio, N.C., Rockne, K.J., Li, A., Peng, H., Tse, T.J., Jones, P.D., Giesy, J.P., 2018b. Spatial and temporal trends in poly- and per-fluorinated compounds in the Laurentian Great Lakes Erie, Ontario and St. Clair. Environmental Pollution 237, 396-405.
Codling, G., Vogt, A., Jones, P.D., Wang, T., Wang, P., Lu, Y.L., Corcoran, M., Bonina, S., Li, A., Sturchio, N.C., Rockne, K.J., Ji, K., Khim, J.S., Naile, J.E., Giesy, J.P., 2014. Historical trends of inorganic and organic fluorine in sediments of Lake Michigan. Chemosphere 114, 203-209.
Dauchy, X., Boiteux, V., Bach, C., Colin, A., Hemard, J., Rosin, C., Munoz, J.-F., 2017. Mass flows and fate of per- and polyfluoroalkyl substances (PFASs) in the wastewater treatment plant of a fluorochemical manufacturing facility. Science of the Total Environment 576, 549-558.
Dauchy, X., Boiteux, V., Rosin, C., Munoz, J.F., 2012. Relationship Between Industrial Discharges and Contamination of Raw Water Resources by Perfluorinated Compounds. Part I: Case Study of a Fluoropolymer Manufacturing Plant. Bulletin of Environmental Contamination and Toxicology 89, 525-530.
Gao, Y., Fu, J., Zeng, L., Li, A., Li, H., Zhu, N., Liu, R., Liu, A., Wang, Y., Jiang, G., 2014. Occurrence and fate of perfluoroalkyl substances in marine sediments from the Chinese Bohai Sea, Yellow Sea, and East China Sea. Environmental Pollution 194, 60-68.
Giesy, J.P., Kannan, K., 2001. Global Distribution of Perfluorooctane Sulfonate in Wildlife. Environmental Science & Technology 35, 1339-1342.
Guo, R., Megson, D., Myers, A.L., Helm, P.A., Marvin, C., Crozier, P., Mabury, S., Bhavsar, S.P., Tomy, G., Simcik, M., McCarry, B., Reiner, E.J., 2016. Application of a comprehensive extraction technique for the determination of poly- and perfluoroalkyl substances (PFASs) in Great Lakes Region sediments. Chemosphere 164, 535-546.
Higgins, C.P., Luthy, R.G., 2006. Sorption of perfluorinated surfactants on sediments. Environmental Science and Technology 40, 7251-7256.
Houde, M., De Silva, A.O., Muir, D.C.G., Letcher, R.J., 2011. Monitoring of Perfluorinated Compounds in Aquatic Biota: An Updated Review. Environmental Science & Technology 45, 7962-7973.
Houde, M., Martin, J.W., Letcher, R.J., Solomon, K.R., Muir, D.C.G., 2006. Biological monitoring of polyfluoroalkyl substances: A review. Environmental Science and Technology 40, 3463-3473.
Kannan, K., 2011. Perfluoroalkyl and polyfluoroalkyl substances: Current and future perspectives. Environmental Chemistry 8, 333-338.
Lafargue, E., Marquis, F., Pillot, D., 1998. Rock-Eval 6 applications in hydrocarbon exploration, production, and soil contamination studies. Revue De L Institut Francais Du Petrole 53, 421-437.
Loi, E.I.H., Yeung, L.W.-Y., Mabury, S.A., Lam, P.K.-S., 2013. Detections of commercial fluorosurfactants in Hong Kong marine environment and human blood: A pilot study. Environmental Science & Technology 47, 4677–4685.
Miège, C., Roy, A., Labadie, P., Budzinski, H., Le Bizec, B., Vorkamp, K., Tronczynski, J., Persat, H., Coquery, M., Babut, M., 2012. Occurrence of priority and emerging organic substances in fishes from the Rhone river in the area of Lyon. Analytical & Bioanalytical Chemistry 4, 2721-2735.
Möller, A., Ahrens, L., Surm, R., Westerveld, J., van der Wielen, F., Ebinghaus, R., de Voogt, P., 2010. Distribution and sources of polyfluoroalkyl substances (PFAS) in the River Rhine watershed. Environmental Pollution 158, 3243-3250.

Muir, D.C.G., Sverko, E., 2006. Analytical methods for PCBs and organochlorine pesticides in environmental monitoring and surveillance: a critical appraisal. Anal. Bioanal. Chem. 386, 769-789.
Munoz, G., Budzinski, H., Labadie, P., 2017a. Influence of Environmental Factors on the Fate of Legacy and Emerging Per- and Polyfluoroalkyl Substances along the Salinity/Turbidity Gradient of a Macrotidal Estuary. Environmental Science & Technology 51, 12347-12357.
Munoz, G., Giraudel, J.-L., Botta, F., Lestremau, F., Dévier, M.-H., Budzinski, H., Labadie, P., 2015. Spatial distribution and partitioning behavior of selected poly- and perfluoroalkyl substances in freshwater ecosystems: A French nationwide survey. Science of the Total Environment 517, 48-56.
Munoz, G., Labadie, P., Botta, F., Lestremau, F., Lopez, B., Geneste, E., Pardon, P., Dévier, M.H., Budzinski, H., 2017b. Occurrence survey and spatial distribution of perfluoroalkyl and polyfluoroalkyl surfactants in groundwater, surface water, and sediments from tropical environments. Science of the Total Environment 607-608, 243-252.
Myers, A.L., Crozier, P.W., Helm, P.A., Brimacombe, C., Furdui, V.I., Reiner, E.J., Burniston, D., Marvin, C.H., 2012. Fate, distribution, and contrasting temporal trends of perfluoroalkyl substances (PFASs) in Lake Ontario, Canada. Environment International 44, 92-99.
Naile, J.E., Khim, J.S., Wang, T., Chen, C., Luo, W., Kwon, B.-O., Park, J., Koh, C.-H., Jones, P.D., Lu, Y., Giesy, J.P., 2010. Perfluorinated compounds in water, sediment, soil and biota from estuarine and coastal areas of Korea. Environmental Pollution 158, 1237-1244.
Paul, A.G., Jones, K.C., Sweetman, A.J., 2009. A First Global Production, Emission, And Environmental Inventory For Perfluorooctane Sulfonate. Environmental Science & Technology 43, 386-392.
Peng, H., Wei, Q., Wan, Y., Giesy, J.P., Li, L., Hu, J., 2010. Tissue distribution and maternal transfer of poly- and perfluorinated compounds in Chinese sturgeon (Acipenser sinensis): Implications for reproductive risk. Environmental Science and Technology 44, 1868-1874.
Poulier, G., Launay, M., Le Bescond, C., Thollet, F., Coquery, M., Le Coz, J., 2019. Combining flux monitoring and data reconstruction to establish annual budgets of suspended particulate matter, mercury and PCB in the Rhone River from Lake Geneva to the Mediterranean Sea. Science of the Total Environment 658, 457-473.
Prevedouros, K., Cousins, I.T., Buck, R.C., Korzeniowski, S.H., 2006. Sources, fate and transport of perfluorocarboxylates. Environmental Science and Technology 40, 32-44.
Stock, N.L., Furdui, V.I., Muir, D.C.G., Mabury, S.A., 2007. Perfluoroalkyl contaminants in the Canadian arctic: Evidence of atmospheric transport and local contamination. Environmental Science and Technology 41, 3529-3536.
Theobald, N., Caliebe, C., Gerwinski, W., Hühnerfuss, H., Lepom, P., 2011. Occurrence of perfluorinated organic acids in the North and Baltic seas. Part 1: distribution in sea water. Environmental Science and Pollution Research, 1-13.
Thompson, J., Roach, A., Eaglesham, G., Bartkow, M.E., Edge, K., Mueller, J.F., 2011. Perfluorinated alkyl acids in water, sediment and wildlife from Sydney Harbour and surroundings. Marine Pollution Bulletin 62, 2869-2875.
Wang, B., Cao, M., Zhu, H., Chen, J., Wang, L., Liu, G., Gu, X., Lu, X., 2013. Distribution of perfluorinated compounds in surface water from Hanjiang River in Wuhan, China. Chemosphere.

Wang, T., Wang, P., Meng, J., Liu, S., Lu, Y., Khim, J.S., Giesy, J.P., 2015. A review of sources, multimedia distribution and health risks of perfluoroalkyl acids (PFAAs) in China. Chemosphere 129, 87-99.
Wang, Y., Arsenault, G., Riddell, N., McCrindle, R., McAlees, A., Martin, J.W., 2009. Perfluorooctane Sulfonate (PFOS) Precursors Can Be Metabolized Enantioselectively: Principle for a New PFOS Source Tracking Tool. Environmental Science & Technology 43, 8283-8289.
Yeung, L.W.Y., De Silva, A.O., Loi, E.I.H., Marvin, C.H., Taniyasu, S., Yamashita, N., Mabury, S.A., Muir, D.C.G., Lam, P.K.S., 2013. Perfluoroalkyl substances and extractable organic fluorine in surface sediments and cores from Lake Ontario. Environment International 59, 389-397.
Zhao, X., Xia, X., Zhang, S., Wu, Q., Wang, X., 2014. Spatial and vertical variations of perfluoroalkyl substances in sediments of the Haihe River, China. Journal of Environmental Sciences 26, 1557-1566.
Zhou, Z., Liang, Y., Shi, Y., Xu, L., Cai, Y., 2013. Occurrence and Transport of Perfluoroalkyl Acids (PFAAs), Including Short-Chain PFAAs in Tangxun Lake, China. Environmental Science & Technology 47, 9249–9257.
Zhou, Z., Shi, Y., Li, W., Xu, L., Cai, Y., 2012. Perfluorinated Compounds in Surface Water and Organisms from Baiyangdian Lake in North China: Source Profiles, Bioaccumulation and Potential Risk. Bulletin of Environmental Contamination and Toxicology 89, 519-524.
Zushi, Y., Tamada, M., Kanai, Y., Masunaga, S., 2010. Time trends of perfluorinated compounds from the sediment core of Tokyo Bay, Japan (1950s-2004). Environmental Pollution 158, 756-763.